Pancreatology 24 (2024) 1257–1264

Contents lists available at ScienceDirect

Pancreatology

journal homepage: www.elsevier.com/locate/pan

Ca^{2+} signaling of pancreatic acinar cells in malignant hyperthermia susceptibility

Nikolett Geyer [a, b], Gyula Diszházi [a], Zsuzsanna É. Magyar [a], Beatrix Dienes [a], Réka Csáki [c], Péter Enyedi [c], Tamara Madácsy [d, e, f], József Maléth [d, e, f], János Almássy [c, *]

[a] Department of Physiology, Faculty of Medicine, University of Debrecen, Debrecen, Hungary
[b] Doctoral School of Molecular Medicine, University of Debrecen, Debrecen, Hungary
[c] Department of Physiology, Semmelweis University, Budapest, Hungary
[d] HCEMM-SZTE Molecular Gastroenterology Research Group, University of Szeged, Szeged, Hungary
[e] Department of Medicine, University of Szeged, Szeged, Hungary
[f] ELKH-USZ Momentum Epithelial Cell Signalling and Secretion Research Group, University of Szeged, Szeged, Hungary

ARTICLE INFO

Article history:
Received 23 August 2024
Received in revised form
30 October 2024
Accepted 3 November 2024
Available online 5 November 2024

Keywords:
Acute pancreatitis
Calcium signaling
Malignant hyperthermia
Ryanodine receptor
Pancreatic acinar cells

ABSTRACT

Background: Malignant hyperthermia susceptibility (MHS) and acute pancreatitis (AP) share a common cellular pathomechanism that is Ca^{2+}-overload of the muscle fiber and the pancreatic acinar cell (PAC). In the muscle, gain-of-function mutations of the ryanodine receptor (RyR1) make the Ca^{2+}-release mechanism hypersensitive to certain ligands, including Ca^{2+}, volatile anaesthetics and succinylcholine, creating a medical emergency when the patient is exposed to these drugs. As RyR1 was shown to contribute to Ca^{2+}-overload in PAC, we presumed that pancreata of MHS individuals are more prone to AP. Accordingly, a recent case study reported coincidence of MHS with recurrent AP, indicating a pathological link between the two diseases.
Methods: We tested if MHS poses a risk for AP in mice carrying the Y522S MHS mutation. Fluorescent Ca^{2+} imaging was performed in PACs. Conventional histopathological analysis and plazma amylase measurement was performed using a cerulein-induced pancreatitis mouse model.
Results: The intracellular Ca^{2+}-signals of PACs from MHS mice were slightly bigger then in wild type when stimulated with 0.2 and 2 μM carbachol (cch) or with 1 and 5 mM bile acid (taurocholic acid). Store-operated-Ca^{2+}-entry was also higher in PACs from MHS mice. Nevertheless, histopathological analysis and plasma amylase levels did not indicate more severe AP in MHS.
Conclusions: These results suggest that the Y522S RyR1 mutation alter the Ca^{2+}-homeostasis in PACs, but not as much as to cause or aggravate AP.

1. Introduction

Gain-of-function mutations of the ryanodine receptor (RyR1) is often associated with uncontrolled Ca^{2+}-release, which is the source of symptoms in certain muscle disorders, such as malignant hyperthermia syndrome (MHS). MHS is an idiosyncratic reaction of the muscle triggered by volatile anaesthetics (halothane, isoflurane, enflurane) and succinylcholine. In susceptible people, anaesthesia increases the resting intracellular calcium ion concentration $[Ca^{2+}]_i$ in skeletal muscle, which causes a generalized muscle contracture. This intense muscle activity progressively raises the body temperature and induces metabolic acidosis and severe hyperkalaemia. If the body is not cooled down and the muscle relaxant dantrolene is not immediately applied, this process leads to death [1,2]. MHS is attributed to point mutations in the RyR sequence, from which 400 have been identified. Early studies have shown that the activating threshold-concentration of volatile anaesthetics is much lower for MHS RyRs compared to wild type therefore, these drugs trigger excessive Ca^{2+}-release in susceptible muscle fibers even at low therapeutic doses. MHS muscle fibres' hypersensitivity has also been demonstrated for other RyR agonists (such as caffeine, 4-chloro-m-cresol, ATP, cADPr) [3–5] and Ca^{2+} induced Ca^{2+} release (CICR) was also found to be higher in MHS muscle [6]. Apparently, agonist-hypersensitivity of MHS RyR is a characteristic

* Corresponding author. 37-47, Tűzoltó st, Budapest, 1094, Hungary.
E-mail address: almassy.janos@semmelweis.hu (J. Almássy).

https://doi.org/10.1016/j.pan.2024.11.005

Abbreviations

RyR	ryanodine receptor
RyR1	skeletal muscle type ryanodine receptor
MHS	malignant hyperthermia syndrome
IP_3	inositol 1,4,5-trisphosphate
IP_3R	inositol 1,4,5-trisphosphate receptor
$[Ca^{2+}]_i$ -	intracellular calcium ion concentration
CICR	Ca^{2+} induced Ca^{2+} release
PAC	pancreatic acinar cell
ACh	acetylcholine
CCK	cholecystokinin
ER	endoplasmic reticulum
FAEE	fatty acid ethyl esters
TLCS	Taurolithocholic acid-3-sulphate
POAEE	palmitoleic acid ethyl ester
TCA	taurocholic acid
CCD	Central Core Disease

feature, explained by impaired interdomain interactions that destabilize the channel's closed state and thus facilitate ligand-gating [7,8]. MHS genotype otherwise does not affect the carrier's everyday life and usually remains undetected.

RyR does not look crucial but has a complementary role in pancreatic acinar cell (PAC) function. PAC secrete digestive enzymes or zymogenes in response to secretagogue stimulation, such as acetylcholine (ACh) and cholecystokinin (CCK). ACh and CCK receptor activation leads to inositol 1,4,5- trisphosphate generation (IP_3), which triggers Ca^{2+}-release from the endoplasmic reticulum (ER) through IP_3 receptor (IP_3R) Ca^{2+}-release channels of the ER membrane. The quality and quantity of fluid- and enzyme secretion of the PAC is determined by the magnitude and spatio-temporal characteristics of the ($[Ca^{2+}]_i$). Low concentrations of stimulants induce oscillations of the $[Ca^{2+}]_i$ highly localized to the apical region, which trigger zymogen exocytosis at the luminal membrane. The apical localization of Ca^{2+}-release is due to the high density of IP_3Rs in this region and to the Ca^{2+} buffering of a mitochondrial belt surrounding this region. At higher, but still physiological secretagogue concentrations Ca^{2+} breaks through the mitochondrial firewall and generates propagating Ca^{2+}-waves, which promote transepithelial fluid secretion too [9–14]. The underlying mechanism of Ca^{2+}-wave propagation is CICR and involves the Ca^{2+}-dependent activation of the RyR. The main RyR isoform in PAC is the same as of skeletal muscle (i.e. RyR1) [15–17].

High concentrations of secretagogues, bile acids, alcohol, and its metabolites (fatty acid ethyl esters, FAEE) induce cell-wide, high amplitude, sustained (peak-plateau) Ca^{2+} signals, which trigger intra-acinar zymogen activation and self-digestion followed by inflammation. This is the initial step of pancreatitis [15,18–20]. Acute pancreatitis is a painful, often deadly disease with a relatively high incidence rate (~10/100000 people/year). The recurrence rate of acute pancreatitis is extremely high (depending on the cause, 10–60 %). The primary cause of the disease is cholelithiasis (gallstones). Due to bile duct obstruction, bile acids may appear in the pancreas or in the systemic circulation in effective concentrations. Another significant risk factor is alcohol abuse, whose damaging effects are mediated by its metabolites, fatty acid ethyl esters (FAEE). Data from Husein's and Petersen's laboratory imply that bile acids and FAEEs trigger excessive Ca^{2+}-release by direct activation of IP_3- and RyR. Taurolithocholic acid-3-sulphate (TLCS) and palmitoleic acid ethyl ester (POAEE) were able to trigger Ca^{2+}-release when IP_3Rs were blocked, but failed when both IP_3R and RyRs were inhibited [15,18–21]. In accordance with these results, our group showed that taurocholic acid (TCA)-induced Ca^{2+}-release was supressed by the RyR-blocker dantrolene and TCA increased the open probability of single RyR channels [22]. In another study from Husein's lab PACs were stimulated by supramaximal doses of the ACh-analogue carbachol and peak $[Ca^{2+}]_i$ was found to be much higher in the RyR-rich basolateral regions compared to the apical. The $[Ca^{2+}]_i$ -difference between the two poles of the cell could be abolished by treatment with ryanodine or dantrolene. Further research demonstrated that cerulein (a CCK analogue) -induced zymogen activation overlapped with the RyR-rich area and dantrolene could mitigate the severity of cerulein-induced pancreatitis. These data provide strong evidence that RyR is important in the pathomechanism of pancreatitis and is a valid therapeutic target [15,19,21].

Since only a minority of heavy drinkers with gallstones develop disease, it is plausible to assume unknown genetic factors in the aetiology of idiopathic pancreatitis. Based on the literature discussed above, it sounds possible that the RyR1 gene is such a genetic factor. Because MHS mutations sensitize RyR to agonists (including Ca^{2+} and bile acids) it is reasonable to hypothesize that MHS mutations are genetic risk factors for acute pancreatitis. The question of this study was whether MHS RyR-expressing PACs are more susceptible for pancreatitis and if they are hypersensitive to the stimulants relevant in pancreatitis aetiology. We tested if ligand-induced Ca^{2+}-transients are more pronounced in MHS PACs. Bile acids and FAEEs don't have a documented malignant hyperthermia trigger potential, although RyRs in skeletal muscle are never exposed to high concentrations of these compounds. Nevertheless, in cholelithiasis, bile acids aggravate the process of pancreatitis, and they may have higher damaging activity in MHS individuals.

The direct motivation to publish our results is a recent case study by Famili et al., reporting on recurrent acute pancreatitis in three patients with RyR1-related myopathy (associated with MHS) [23]. Based on the *in vitro* data –that the gain-of-function mutations create a leaky channel phenotype which may lead to excessive RyR-mediated Ca^{2+} -release and lower the threshold for pathological PAC stimulation –, the authors argue that the association of the two rare diseases in these patients is causative and not only a rare coincidence. Patient #1 was diagnosed with Central Core Disease (CCD) and MHS due to a heterozygous dominant RyR1 mutation, c.14818G > A; p.Ala4940Thr, Patient #2 had King-Denborough Syndrome (KDS) and MHS due to a heterozygous dominant RyR1 mutation (c.7354C > T; p.Arg2452Trp), a common MHS-associated variant and Patient #3 had a family history of MH and he suffered from Exertional Heat Illness and debilitating muscle spasms. His MHS was not genetically identified but was confirmed by Caffeine Halothane Contracture Test. RyR-related disorders manifest in a wide range of severity of conditions ranging from asymptomatic to severe disability [23]. Based on the descriptions, the reported three patients represent mild to severe cases.

In the current study, we investigated the hypothesis that the MHS RyR phenotype may contribute to pathological Ca^{2+}-overload in pancreatic acinar cells. To this, Ca^{2+} signalling of pancreatic acinar cells isolated from Y522S RyR1 knock-in mice were tested and compared to control [6,24]. It should be noted that the symptoms of these mice of young age most closely resemble to those of patient 3. Later, central, clear cores in muscle fibres, a hallmark of Central Core Disease (CCD) also occur, but in discrete areas ("presumptive cores"), which gradually progresses to the typical histopathological image of CCD., Y522S mutation is also linked to severe CCD, in humans too, like patient #1.

2. Material and methods

The methods were conducted in accordance with the ARRIVE guidelines. All methods were performed in accordance with the relevant guidelines and regulations.

2.1. Animals

All animal studies were designed to minimize animal suffering and were performed in accordance with EU (86/609/EEC) guideline under a license obtained from the Scientific Committee on Animal Health and Welfare of the University of Debrecen (11/2015/DEMÁB). 10–16-weeks-old, heterozygous RyR1 Y522S MHS knock-in Bl6 mice and their control littermates were used in this study [24]. (The homozygous mice die at the pre-perinatal period.) This strain was kindly provided by Susan L Hamilton (Baylor College of Medicine) and Werner Melzer (Ulm University). The heterozygous mice show MH phenotype and the muscle's pathology have already been well characterized [6,24,25–29], and was found to be equivalent to the human phenotype. Genotyping was performed by an established PCR protocol. Mice were euthanized by CO_2 asphyxiation.

2.2. Pancreatic acinar cell isolation

Acinar cell isolation was performed as described earlier [17,22]. Briefly, pancreata ($n \geq 3$/each group) were enzymatically digested with type-II collagenase in minimum essential medium and 1 mg/mL trypsin inhibitor for 30 min at 37 °C, followed by gentle trituration using a serological pipette. Acinar cells were then filtered through 100 μm nylon mesh, centrifuged at 75×*g*, and resuspended in 1 % BSA minimum essential medium [17,22].

2.3. Ca^{2+} imaging of native pancreatic acinar cells

Cells were seeded onto #1 glass coverslips and loaded with 4 μM Fluo-4 AM for 20 min at room temperature in a linear-flow perfusion chamber. The chamber was mounted onto the stage of an LSM 510 or LSM-Live laser scanning confocal microscope. The cells were washed with physiological HEPES buffered saline solution (130 mM NaCl, 5 mM KCl, 10 mM HEPES, 2 mM $CaCl_2$, 2 mM $MgCl_2$, pH = 7.38) and experiments ($N \geq 3$) were performed on small clumps of acinar cells with pronounced polarized apical secretory granule localization. The Ca^{2+}-free bath solution was similar, but with no added Ca^{2+}, and with 0.5 mM EGTA. Agonist-induced elevations of the intracellular calcium ion concentration ($[Ca^{2+}]i$) was monitored through Fluo-4 fluorescence. The specimen was illuminated with 488 nm laser light and the emitted fluorescence was collected through a 510 nm band-pass filter [22].

2.4. Induction and evaluation of acute pancreatitis

Acute pancreatitis was induced by repetitive intraperitoneal cerulein injections. The mice (wt group n = 7 and MHS group n = 8) received 100 mg/bwkg cerulein (in physiological saline) injections 2–7 times hourly, depending on the experimental design. The animals were sacrificed 1 h after the last injection. The severity of pancreatic injury was assessed by measuring amylase activity of the blood plasma, in two sets of experiments: after 2 cerulein injections or 6 injections, respectively. Blood samples were taken from the heart of the mice and collected in EGTA-containing vials. Amylase activity of the plasma was determined using an amylase assay kit (Sigma-Aldrich) according to the manufacturer's instructions.

Another cohort of wt and MHS (n = 7 and 8) mice were treated with cerulein 7 times and were sacrificed 1 day after the first injection (to allow longer time for the development of pancreatic tissue injury). The pancreata of these animals were removed and immediately fixed in formalin. The tissue was processed using a conventional histological procedure followed by hematoxilin and eosin staining.

3 tissue sections from each mice were evaluated by 3 investigators by observing multiple microscope fields [30,31]. The severity of the symptoms of pancreatitis were evaluated using a scale of 0–5 or 0–100 %, respectively. For oedema, 0: none; 1: slight patchy interlobular; 2: patchy interlobular 3: diffuse interlobular; 4: patchy interlobular and intra-acinar 5: diffuse interlobular and intra-acinar, for leukocyte infiltration: 0: none; 1: diffuse/slight; 2: diffuse/mild; 3: diffuse/moderate; 4: diffuse/severe 5: diffuse/very severe. For necrosis, the percentage of the necrotic area was assessed.

2.5. Statistics

Statistical analysis was performed in Origin 7.0 (OriginLab, Northampton, MA) and in Excel (Microsoft, Redmond, WA). Results are expressed as mean ± SE. Statistical significance of differences was evaluated using independent two-sample *t*-test or Mann-Whitney test. Differences were considered significant when the *p*-value was less than 0.01 and labelled with asterisk (*) in the figures. The number of cells (or mice in Fig. 4) investigated is given in the figures in brackets.

3. Results

The ultimate question of the current research was, if MHS could be or could not be a genetic risk factor for pancreatitis. To this end first, mouse pancreatic acinar cells (PAC) were isolated enzymatically and used in Ca^{2+}-imaging experiments. We tested whether PACs from Y522S RyR1 mice were more susceptible to the stimulation with the cholinomimetic drug carbachol, and whether they were more affected by bile acids compared to PACs from wild-type (wt) littermates. It should be noted that these compounds are physiologically or pathologically relevant stimulants of Ca^{2+} signaling in pancreatic acinar cells [18,20]. The temporal characteristics (shape, pattern) and amplitude of the Ca^{2+} signals were evaluated. We found that physiologically relevant concentrations of carbachol (50, 100 and 250 nM) induced repetitive fluctuations of the $[Ca^{2+}]_i$, in both wild type and MHS acinar cells. The amplitude of these responses were not different in the two groups in 50 nM cch (ΔF WT = 429 ± 25, ΔF MHS = 371 ± 38), while they were higher in 200 nM (ΔF WT = 455 ± 26, ΔF MHS = 776 ± 29), at which RyRs are believed to be involved in the process (see an example for fluorimetric traces in Fig. 1A). Average fluorescence amplitudes are presented in Fig. 1B. Importantly, the temporal pattern of Ca^{2+} signals was similar in MHS and wt that is, a shift toward a peak-plateau-type response (i.e. a sign of Ca^{2+}-overload) was not observed. At the end of each experiment, supramaximal dose of cch (2 μM) was applied to demonstrate the maximal response. The absolute values of these amplitudes were lower due to photobleaching, but they lost the oscillatory characteristic, and they were higher in MHS (ΔF WT = 329 ± 16, ΔF MHS = 411 ± 15).

Similar experiments were performed using 1 and 5 mM TCA in a Ca^{2+}-free medium (1 mM being a ~threshold concentration) (Fig. 2) [22]. Both concentrations induced Ca^{2+} signals of an oscillatory fashion, but the amplitudes were substantially higher in 5 mM TCA (Fig. 2A and D). In both TCA concentrations, the pattern, and the average amplitude were similar in MHS PACs compared to wt (ΔF WT $_{1mM\ TCA}$ = 218 ± 14; ΔF MHS $_{1mM\ TCA}$ = 223 ± 14; ΔF WT $_{5mM\ TCA}$ = 312 ± 18; ΔF MHS $_{5mM\ TCA}$ = 341 ± 19) (Fig. 2B and E). The area under the curves (AUC) - which correlates with the amount of Ca^{2+}

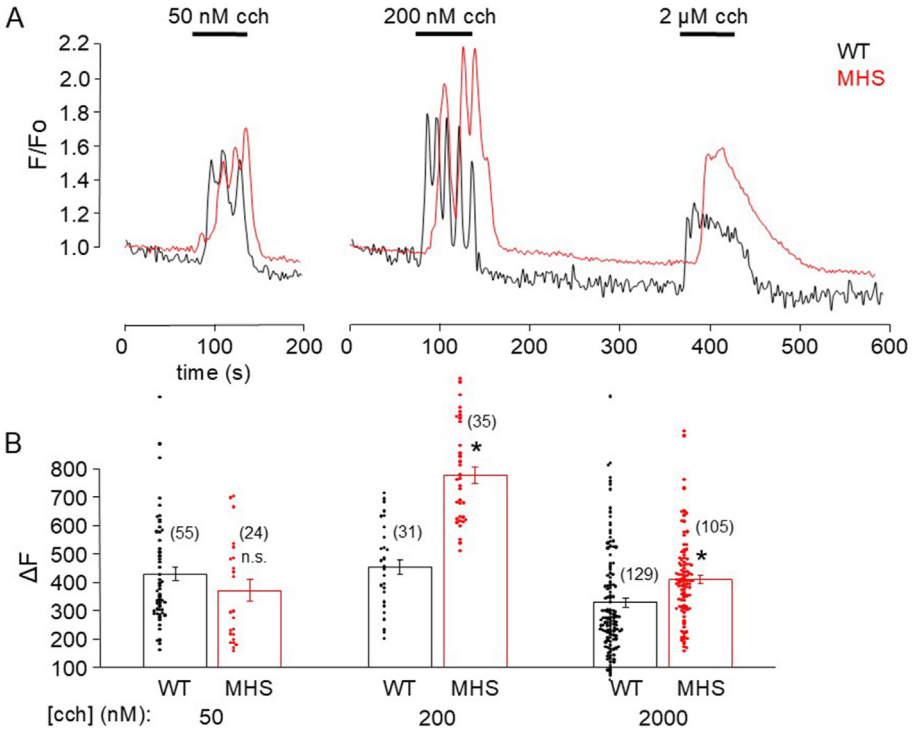

Fig. 1. *Intracellular Ca^{2+} signal responses to carbachol in pancreatic acinar cells isolated from malignant hyperthermia susceptible (MHS) and wild type (WT) mice*
Intracellular Fluo-4 fluorescence normalized to the baseline intracellular fluorescence (F/F_0) was plotted as the function of time. Acinar cells were treated with 50, 200 nM and 2 µM carbachol (cch) for 90 s, subsequently (A). Average changes of peak fluorescence (ΔF) and individual data points (B). (n.s. – not significant, * – $p < 0.01$).

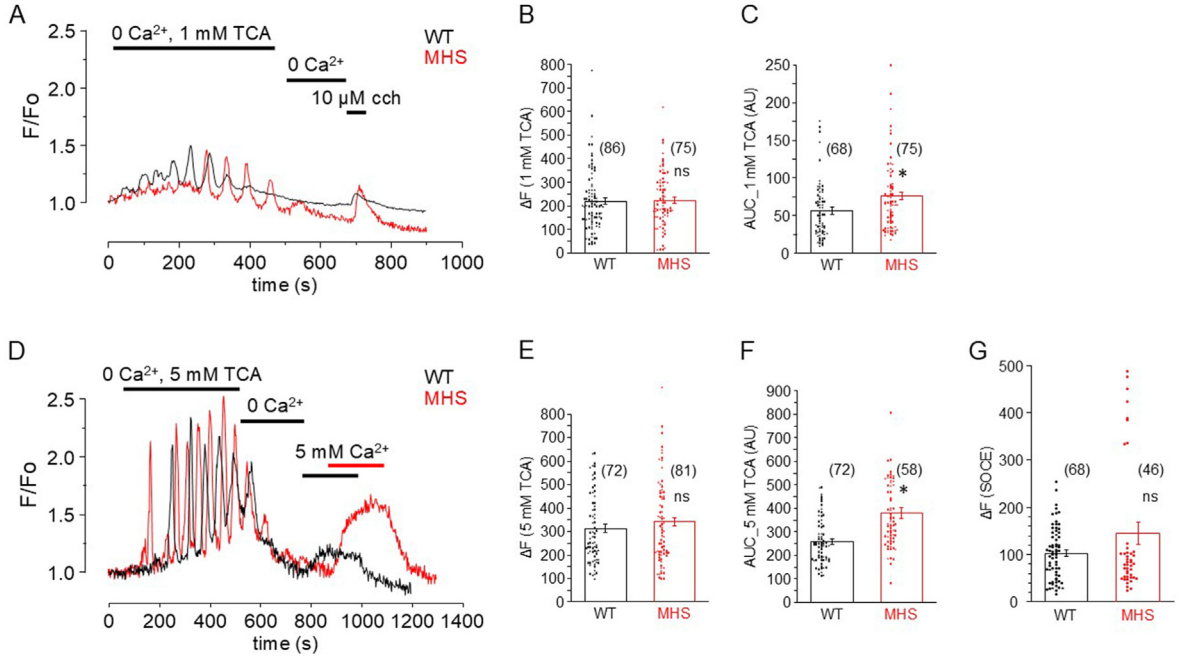

Fig. 2. *Intracellular Ca^{2+} signal responses to the bile acid taurocholic acid (TCA) in pancreatic acinar cells from malignant hyperthermia susceptible (MHS) and wild type mice*
Acinar cells were treated with 1 mM TCA in Ca^{2+} free solution for 4 min, which was followed by 10 µM carbachol (cch) (A). Acinar cells stimulated by 5 mM TCA, followed by 5 mM Ca^{2+} at 11 min (B). Intracellular Fluo-4 fluorescence was normalized to the baseline intracellular fluorescence (F/F_0) and plotted as the function of time. The amplitude of fluorescence change (ΔF) was determined from the Fluo-4 fluorescence intensity and shown in B an E. Area under the curve (AUC) of fluorescence oscillartions in 1 and 5 mM TCA are expressed in arbitrary units (AU) in panel C and F, respectively. (n.s. – not significant, * – $p < 0.01$). ΔF in 5 mM Ca^{2+} (SOCE) is shown in panel G. Individual data points are also displayed.

released - was slightly, but statistically significantly bigger in the case of MHS at both TCA concentrations (AUC WT $_{1mM\ TCA} = 56 \pm 5$; AUC MHS $_{1mM\ TCA} = 76 \pm 5$; AUC WT $_{5mM\ TCA} = 260 \pm 12$; AUC MHS $_{5mM\ TCA} = 380 \pm 23$) (Fig. 2C and F). TCA was applied long enough to

trigger store-operated Ca^{2+}-entry (SOCE), which was apparent when 5 mM Ca^{2+} was added in the extracellular medium (Fig. 2D). SOCE-related Ca^{2+} signal was considerably higher in MHS, (Fig. 2G). (Similar experiments have been performed using another bile acid taurolithocolic acid sulphate (TLCS), with qualitatively same results: ΔF SOCE WT = 135 ± 10 and ΔF SOCE MHS = 174 ± 10).

Therefore, SOCE was investigated more systematically in next experiments, which were designed to be more suitable for assessing the ER Ca^{2+} load and SOCE as well. To this end, cells were treated with the SERCA pump inhibitor thapsigargin (TG) to empty the intracellular Ca^{2+} stores in Ca^{2+}-free medium (Fig. 3A). The dynamics and the amplitude of the resulting Ca^{2+}-signals were evaluated. The Ca^{2+}-release rate (slope) in MHS was steeper, but similar amplitude as in the control (ΔF_{TG} WT = 492 ± 42; ΔF_{TG} MHS = 470 ± 21) (Fig. 3C and B). Nevertheless, the area under the curve (AUC) was significantly lower (−19 %) in MHS (AUC WT $_{SOCE}$ = 267 ± 10; AUC MHS $_{SOCE}$ = 224 ± 12) (Fig. 3D). These data indicate that the ER's Ca^{2+} content is slightly lower (partial depletion) in MHS acinar cells, the Ca^{2+} stores deplete more rapidly, but the approachable Ca^{2+} peak is the same in MHS. These results raise the question whether the activity of SOCE is different in the two groups. As SOCE is known to be a critical Ca^{2+} entry pathway during the pathogenesis of acute pancreatitis and store-operated current inhibitors mitigated the severity of pancreatitis in mice, this is a particularly important question [30–33]. It is reasonable to assume that the leaky channel phenotype (lower store load and enhanced Ca^{2+} release) of MHS RyR, may secondarily affect SOCE. To answer this, following the store depletion with TG in Ca^{2+}-free bath, cells were superfused with a medium supplemented with 5 mM Ca^{2+} (Fig. 3A). MHS cells showed significantly higher Ca^{2+} elevation compared to wt (204 ± 20 vs. 136 ± 16, p = 0.0003, Mann-Whitney test), which indicates that the Ca^{2+} entry pathways are more active in MHS (Fig. 3E). Because SOCE also significantly contributes to bile acid induced Ca^{2+} overload during the early stage of acute pancreatitis, the magnitude of Ca^{2+} entry after TCA treatment was also evaluated, which was 103 ± 7 and 144 ± 24, which is somewhat higher in MHS, but statistically not different (Fig. 2G). The possible reason why the TG-evoked SOCE was significantly different in MHS while the TCA-evoked SOCE was not, is that in the TCA experiments SERCA activity was not inhibited during the Ca^{2+} influx (TCA was washed out by this time), which allowed for a partial compensation of the higher Ca^{2+} entry in MHS while in the TG-experiments this effect did not take place because of the constant presence of TG.

To answer the ultimate question of this project, whether MHS is a risk factor of pancreatitis, a mouse pancreatitis model was generated. Mice were injected several times hourly with 100 mg/kg body weight cerulein. The severity of pancreatic injury was assessed by measuring amylase activity of the plasma. In initial experiments, even 2 cerulein-treatment induced significant elevation of plasma amylase activity, no difference was observed between control and MHS groups (3051 ± 87 and 2892 ± 426 AU, n = 4) (Fig. 4A). To induce more severe pancreatic injury, similar experiment was performed with 6 consecutive injections, with

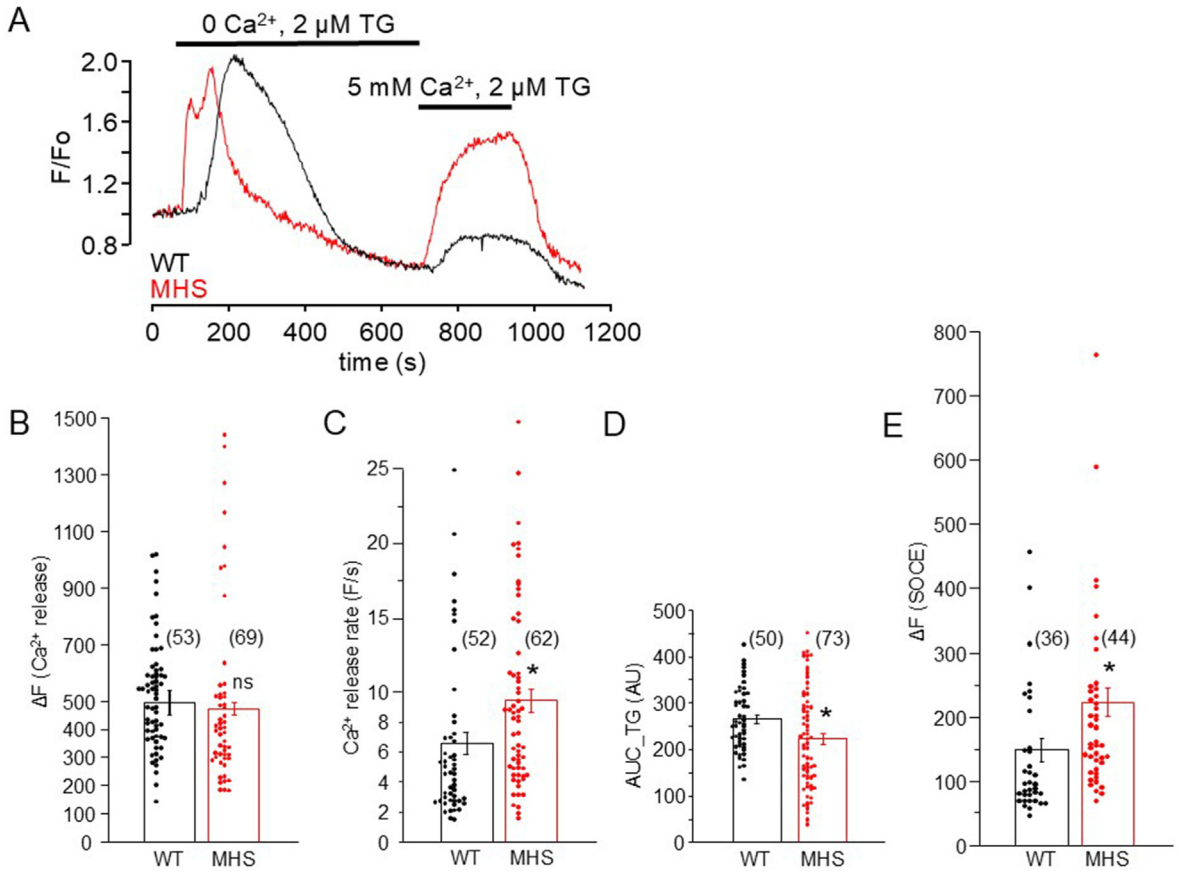

Fig. 3. *Ca^{2+} response of pancreatic acinar cells to the SERCA pump inhibitor thapsigargin (TG) in Ca^{2+}-free and* 5 mM *Ca^{2+} containing extracellular media*
The endoplasmic reticulum was emptied by triggering Ca^{2+}-release by using TG in Ca^{2+} free bath. Ca^{2+} addition was followed by an increase in the intracellular Ca^{2+} concentration, due to store-operated Ca^{2+}-entry (SOCE) (A). The mean amplitude and the rate (slope) of the initial Ca^{2+}-release is shown in B and C, respectively. The area under the TG-induced fluorescence curve is shown in D. Fluorescence intensity change (ΔF) during SOCE is in E. (n.s. – not significant, * – p < 0.01). Individual data points are also displayed.

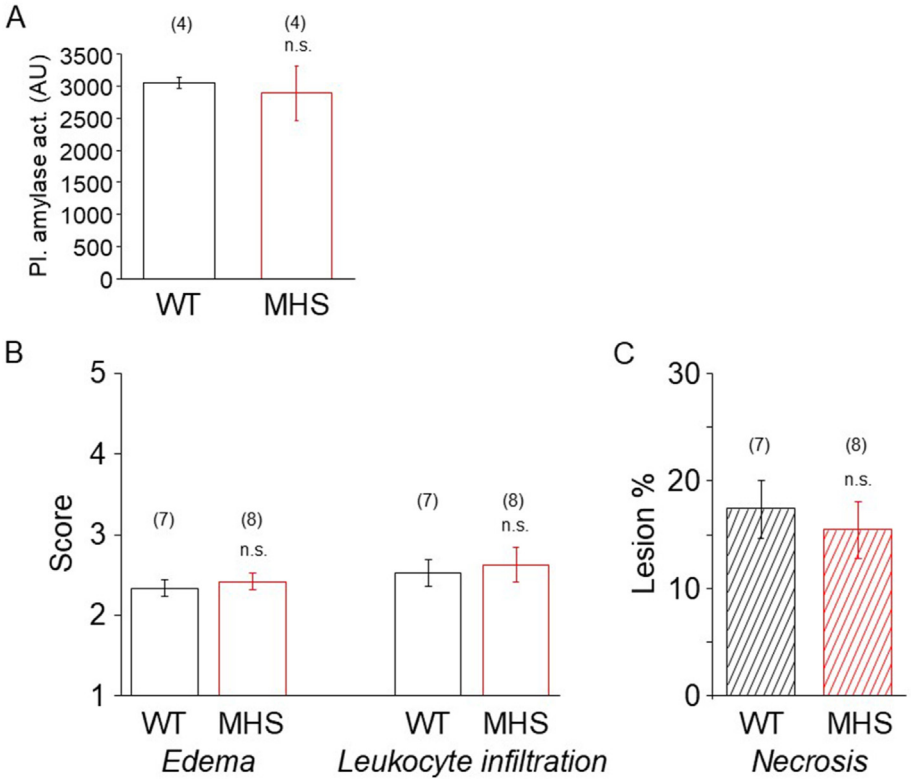

Fig. 4. *Histopathology of pancreatic injury in cerulein-induced acute pancreatitis*
Plasma amylase activity of wt and MHS mice are shown in A.
Histological scoring of oedema and leukocyte infiltration was assessed using a scale ranging from 0 to 5 (B). Pancreatic injury was determined as the percentage of necrotic area (C). (n.s. – not significant).

very similar results.

In other experiments, mice were treated with cerulein 7 times and were sacrificed 1 day later. Their pancreata were removed and after conventional histochemical preparations, pancreatic slices were stained with hematoxilin-eosin. The severity of the symptoms of pancreatitis were evaluated using a scale of 0–5 or 0–100 %, respectively. Tissue oedema scored 2.33 ± 0.1 in control vs. 2.42 ± 0.1 of MHS, leukocyte infiltration was 2.52 ± 0.16 vs. 2.63 ± 0.21 and necrosis was 17.4 ± 2.7 vs. 15.4 ± 2.6 %, suggesting that MHS do not increase the susceptibility of mice for pancreatic injury and pancreatitis (Fig. 4B and C).

4. Discussion

The motivation to share our results here was a paper published by Famili et al. few months ago reporting on three cases of pancreatitis in patients with RyR-related myopathy (MHS), suggesting a link between the two diseases [23]. Our results of histological analysis did not confirm the hypothesis that a RyR mutation would be a risk factor of acute pancreatitis (at least in Y522S) however, Ca^{2+} imaging data showed mild, but statistically significant alteration of Ca^{2+} signalling in PACs. As it is important to learn if the co-occurrence of the two diseases is a mere coincidence or comorbidity, this piece of information is relevant.

In summary, our results suggest that in the physiologically and pathologically relevant concentration range of carbachol (200 nM and 2 μM) and TCA, RyR1's deficiency is relevant enough to alter and the magnitude of Ca^{2+} signals, suggesting that RyR1 contributes to Ca^{2+} release and the "leaky" phenotype is uncompensated by Ca^{2+} clearance at strong stimulations. Important to highlight is that the temporal characteristics (dynamics and pattern) of the Ca^{2+}-signals did not show a pathological deviation in the direction of peak-plateau-type Ca^{2+} signals, a hallmark of toxic Ca^{2+} overload. At low (50 nM) carbachol, the amplitudes were similar in the two groups, consistent with the fact that this concentration evokes apically localized Ca^{2+} elevations, where RyRs are believed not to contribute to the process.

Consistent with the leaky and hypersensitive phenotype of RyR1, the ER Ca^{2+} store was partially depleted, but this apparently, did not limit the releasable amount of $[Ca^{2+}]_i$, as the Ca^{2+} release rate and total Ca^{2+} released was higher in MH. In addition, our experiments revealed a secondary consequence of the "leaky" phenotype of RyR at the cellular level, that is the ER load was slightly lower and emptied faster in MHS, resulting in an enhanced SOCE. But SOCE was significantly higher only under special experimental conditions, when the SERCA pump was inhibited (in TG), implying that the consequences of RyR disfunction are most likely compensated by Ca^{2+} clearance mechanisms. Thus, Ca^{2+} overload during pathological overstimulation of the pancreas is slightly bigger in MHS then in wild type. Consistent with this result, a more severe manifestation of acute pancreatitis in MHS in a cerulein overstimulation mouse model could not be observed.

Although, others demonstrated RyR to be a relevant player in the pathogenesis of pancreatitis and we previously showed that bile acids directly activate RyRs (in addition to IP_3Rs) and that RyR contributes to the development of pathological Ca^{2+} signals [15,19,21,22], our current results imply that RyR disfunction alone has only a minor additional pathogenic role. MHS RyR did not make the pathological condition worse, probably because its leakiness is compensated by Ca^{2+} elimination. This conclusion is also supported by our earlier study, showing that the RyR1/IP_3R expression ratio is low in the pancreas [17]. Compared to the muscle, where

RyR is the only and highly abundant Ca^{2+} release channel in the SR membrane, a relatively significant Ca^{2+} leak neither cause a muscle problem under baseline conditions, as it is compensated. The consequence of enhanced leak is manifested only under anaesthesia.

4.1. Limitations of the study

The secretagogues in this study were not fully investigated, as the effect of CCK, which would correlate more closely with results from the cerulein-induced pancreatitis model, was not examined by Ca^{2+} imaging. Additionally, using an obstruction-induced model could have been justified. Thus, these results are rather preliminary.

Although the Y522S mutation tested in this study is a strong phenotypic mutation linked to MH and CCD, similar in severity to patient 3 and patient 1, a limitation is that only one transgenic mouse strain was tested (of four existing MH/CCD strains). This limits generalizability, leaving open the possibility that Y522S is not human-pathologically relevant and that the association of other RyR mutations with pancreatitis might have been confirmed.

5. Conclusions

In conclusion, our results suggest that the Y522S RyR1 mutation alter the Ca^{2+}-homeostasis in PACs, but not as much as to cause or aggravate AP. The temporal characteristics of Ca2+ signals did not deviate toward pathological, peak-plateau shape. All in all, we did not find a link between Y522S RyR and pancreatitis, thus we conclude that this mutation does not increase the risk for acute pancreatitis. We propose that increased pancreatitis propensity is not a general feature of all the RyR-related disorders. It is important to note that these data do not exclude the possibility that some more severe gain-of-function RyR mutations may be a direct pathogenic factor in pancreatic disease. Unfortunately, databases (such as the UK biobank or Genome-wide association studies) do not contain enough cases to allow correlation analysis between these two rare diseases. Nevertheless, the hypothesis of RyR-related pancreatitis is not supported by post-operative observations either, as acute pancreatitis or other pancreatic complications have never been reported after MH episodes. The recently reported cases of pancreatitis in RyR-related disorders being either rare cases or bare coincidence, they call our attention to a possible pathological link which should be further investigated.

Author contributions

Nikolett Geyer: investigation (equal), Formal analysis (equal); visualization (equal); writing—review and editing (equal). Gyula Diszházi: methodology (supporting). Zsuzsanna É Magyar: methodology (supporting). Beatrix Dienes: writing—review and editing (supporting). Réka Csáki: Formal analysis (supporting). Péter Enyedi: writing—review and editing (supporting). Tamara Madácsy: investigation (equal). József Maléth: investigation (equal). János Almássy: Conceptualization (equal); funding acquisition (equal); resources (equal); supervision (equal); investigation (equal), Formal analysis (equal); visualization (equal); writing—original draft (equal); writing—review and editing (equal).

Data availability statement

All study data are included in the article. Data are available on request from the corresponding author, János Almássy.

Competing interests statement

The authors declare no conflict of interest.

Acknowledgements

The authors appreciate the excellent technical assistance of József Orosz.

This work was funded by the National Research Development and Innovation Fund of Hungary provided to J.A. (NKFIH PD112199 and FK144576) J.A and T.M. are supported by the Janos Bolyai Research Scholarship of the Hungarian Academy of Sciences. J.A.'s and T.M.'s work was supported by the New National Excellence Program (ÚNKP-23-5.) of the Ministry for Innovation and Technology of Hungary.

This project had been implemented with the support provided by the Ministry of Innovation and Technology of Hungary from the National Research Development and Innovation Fund, financed under the TKP2021-EGA funding scheme (TKP2021-EGA-24).

References

[1] MacLennan DH, Phillips MS. Malignant hyperthermia. Science 1992;256(5058):789–94. https://doi.org/10.1126/science.1589759.
[2] Kolb ME, Horne ML, Martz R. Dantrolene in human malignant hyperthermia A multicenter study. Anesthesiology 1982;56(4):254–62. https://doi.org/10.1097/00000542-198204000-00005.
[3] Zucchi R, Ronca-Testoni S. The sarcoplasmic reticulum Ca2+ channel/ryanodine receptor: modulation by endogenous effectors, drugs and disease states. Pharmacol Rev 1997;49(1):1–51.
[4] Dulhunty AF, Beard NA, Pouliquin P, Kimura T. Novel regulators of RyR Ca2+ release channels: insight into molecular changes in genetically-linked myopathies. J Muscle Res Cell Motil 2006;27(5–7):351–65. https://doi.org/10.1007/s10974-006-9086-1.
[5] Mickelson JR, Litterer LA, Jacobson BA, Louis CF. Stimulation and inhibition of [3H]ryanodine binding to sarcoplasmic reticulum from malignant hyperthermia susceptible pigs. Arch Biochem Biophys 1990;278(1):251–7. https://doi.org/10.1016/0003-9861(90)90255-w.
[6] Durham WJ, Aracena-Parks P, Long C, et al. RyR1 S-nitrosylation underlies environmental heat stroke and sudden death in Y522S RyR1 knockin mice. Cell 2008;133(1):53–65. https://doi.org/10.1016/j.cell.2008.02.042.
[7] Tung CC, Lobo PA, Kimlicka L, Van Petegem F. The amino-terminal disease hotspot of ryanodine receptors forms a cytoplasmic vestibule. Nature 2010;468(7323):585–8. https://doi.org/10.1038/nature09471.
[8] Kimlicka L, Lau K, Tung CC, Van Petegem F. Disease mutations in the ryanodine receptor N-terminal region couple to a mobile intersubunit interface. Nat Commun 2013;4(1):1506. https://doi.org/10.1038/ncomms2501.
[9] Yule DI, Stuenkel E, Williams JA. Intercellular calcium waves in rat pancreatic acini: mechanism of transmission. Am J Physiol 1996;271(4 Pt 1):C1285–94. https://doi.org/10.1152/ajpcell.1996.271.4.C1285.
[10] Petersen OH, Findlay I, Iwatsuki N, et al. Human pancreatic acinar cells: studies of stimulus-secretion coupling. Gastroenterology 1985;89(1):109–17. https://doi.org/10.1016/0016-5085(85)90751-6.
[11] Tinel H, Cancela JM, Mogami H, et al. Active mitochondria surrounding the pancreatic acinar granule region prevent spreading of inositol trisphosphate-evoked local cytosolic Ca(2+) signals. EMBO J 1999;18(18):4999–5008. https://doi.org/10.1093/emboj/18.18.4999.
[12] Straub SV, Giovannucci DR, Yule DI. Calcium wave propagation in pancreatic acinar cells: functional interaction of inositol 1,4,5-trisphosphate receptors, ryanodine receptors, and mitochondria. J Gen Physiol 2000;116(4):547–60. https://doi.org/10.1085/jgp.116.4.547.
[13] Toescu EC, Lawrie AM, Petersen OH, Gallacher DV. Spatial and temporal distribution of agonist-evoked cytoplasmic Ca2+ signals in exocrine acinar cells analysed by digital image microscopy. EMBO J 1992;11(4):1623–9. https://doi.org/10.1002/j.1460-2075.1992.tb05208.x.
[14] Thorn P, Lawrie AM, Smith PM, Gallacher DV, Petersen OH. Local and global cytosolic Ca2+ oscillations in exocrine cells evoked by agonists and inositol trisphosphate. Cell 1993;74(4):661–8. https://doi.org/10.1016/0092-8674(93)90513-p.
[15] Orabi AI, Shah AU, Ahmad MU, et al. Dantrolene mitigates caerulein-induced pancreatitis in vivo in mice. Am J Physiol Gastrointest Liver Physiol 2010;299(1):G196–204. https://doi.org/10.1152/ajpgi.00498.2009.
[16] Ashby MC, Petersen OH, Tepikin AV. Spatial characterisation of ryanodine-induced calcium release in mouse pancreatic acinar cells. Biochem J 2003;369(Pt 3):441–5. https://doi.org/10.1042/BJ20021039.
[17] Diszházi G, Magyar ZÉ, Lisztes E, et al. TRPM4 links calcium signaling to membrane potential in pancreatic acinar cells. J Biol Chem 2021;297(3):101015. https://doi.org/10.1016/j.jbc.2021.101015.

[18] Gerasimenko JV, Flowerdew SE, Voronina SG, et al. Bile acids induce Ca2+ release from both the endoplasmic reticulum and acidic intracellular calcium stores through activation of inositol trisphosphate receptors and ryanodine receptors. J Biol Chem 2006;281(52):40154–63. https://doi.org/10.1074/jbc.M606402200.
[19] Husain SZ, Orabi AI, Muili KA, et al. Ryanodine receptors contribute to bile acid-induced pathological calcium signaling and pancreatitis in mice. Am J Physiol Gastrointest Liver Physiol 2012;302(12):G1423–33. https://doi.org/10.1152/ajpgi.00546.2011.
[20] Gerasimenko JV, Lur G, Sherwood MW, et al. Pancreatic protease activation by alcohol metabolite depends on Ca2+ release via acid store IP3 receptors. Proc. Natl. Acad. Sci. U.S.A 2009;106(26):10758–63. https://doi.org/10.1073/pnas.0904818106.
[21] Husain SZ, Prasad P, Grant WM, Kolodecik TR, Nathanson MH, Gorelick FS. The ryanodine receptor mediates early zymogen activation in pancreatitis. Proc Natl Acad Sci U S A 2005;102(40):14386–91. https://doi.org/10.1073/pnas.0503215102.
[22] Geyer N, Diszházi G, Csernoch L, Jóna I, Almássy J. Bile acids activate ryanodine receptors in pancreatic acinar cells via a direct allosteric mechanism. Cell Calcium 2015;58(2):160–70. https://doi.org/10.1016/j.ceca.2015.03.009.
[23] Famili DT, Mistry A, Gerasimenko O, et al. Pancreatitis in RYR1-related disorders. Neuromuscul Disord 2023;33(10):769–75. https://doi.org/10.1016/j.nmd.2023.09.003.
[24] Chelu MG, Goonasekera SA, Durham WJ, et al. Heat- and anesthesia-induced malignant hyperthermia in an RyR1 knock-in mouse. Faseb J 2006;20(2):329–30. https://doi.org/10.1096/fj.05-4497fje.
[25] Boncompagni S, Rossi AE, Micaroni M, et al. Characterization and temporal development of cores in a mouse model of malignant hyperthermia. Proc Natl Acad Sci U S A 2009;106(51):21996–2001. https://doi.org/10.1073/pnas.0911496106.
[26] Corona BT, Hamilton SL, Ingalls CP. Effect of prior exercise on thermal sensitivity of malignant hyperthermia-susceptible muscle. Muscle Nerve 2010;42(2):270–2. https://doi.org/10.1002/mus.21715.
[27] Lanner JT, Georgiou DK, Dagnino-Acosta A, et al. AICAR prevents heat-induced sudden death in RyR1 mutant mice independent of AMPK activation. Nat Med 2012;18(2):244–51. https://doi.org/10.1038/nm.2598.
[28] Andronache Z, Hamilton SL, Dirksen RT, Melzer W. A retrograde signal from RyR1 alters DHP receptor inactivation and limits window Ca2+ release in muscle fibers of Y522S RyR1 knock-in mice. Proc. Natl. Acad. Sci. U.S.A 2009;106(11):4531–6. https://doi.org/10.1073/pnas.0812661106.
[29] Manno C, Figueroa L, Royer L, et al. Altered Ca2+ concentration, permeability and buffering in the myofibre Ca2+ store of a mouse model of malignant hyperthermia. J Physiol 2013;591(18):4439–57. https://doi.org/10.1113/jphysiol.2013.259572.
[30] Pallagi P, Görög M, Papp N, et al. Bile acid- and ethanol-mediated activation of Orai1 damages pancreatic ductal secretion in acute pancreatitis. J Physiol 2022;600(7):1631–50. https://doi.org/10.1113/JP282203.
[31] Szabó V, Csákány-Papp N, Görög M, et al. Orai1 calcium channel inhibition prevents progression of chronic pancreatitis. JCI Insight 2023;8(13). https://doi.org/10.1172/jci.insight.167645.
[32] Wen L, Voronina S, Javed MA, et al. Inhibitors of ORAI1 prevent cytosolic calcium-associated injury of human pancreatic acinar cells and acute pancreatitis in 3 mouse models. Gastroenterology 2015;149(2):481–492.e7. https://doi.org/10.1053/j.gastro.2015.04.015.
[33] Gerasimenko JV, Gryshchenko O, Ferdek PE, et al. Ca2+ release-activated Ca2+ channel blockade as a potential tool in antipancreatitis therapy. Proc. Natl. Acad. Sci. U.S.A 2013;110(32):13186–91. https://doi.org/10.1073/pnas.1300910110.